A Putative ATP-Activated Na^+ Channel Involved in Sperm-Induced Fertilization

Yuval Kupitz and Daphne Atlas*

Extracellular application of adenosine triphosphate (ATP) to defolliculated *Xenopus laevis* oocytes activated a saturating inward current with a maximal amplitude E_{max} of 2.4 ± 0.2 microamperes and an apparent Michaelis constant of 197.6 micromolar. The current was carried predominantly by sodium ions and potently inhibited by amiloride, guanosine triphosphate (GTP), and its nonhydrolyzable analogs guanosine 5′-[β,γ-imido]triphosphate (GppNHp) and guanosine 5′-*O*-(3-thiotriphosphate). Likewise, in vitro fertilization using mature eggs and *Xenopus* sperm was inhibited by amiloride, GTP, and GppNHp. Hence, an ATP receptor on the egg membrane may be the recipient target for ATP originating in sperm, suggesting that an ATP-induced increase in sodium permeability mediates the initial sperm to egg signal in the fertilization process.

The generation of a fertilization potential is the earliest response of sperm to egg in a variety of species (*1, 2*). The rapid positive shift in the membrane potential of the egg is caused by an increase in Na^+ permeability that appears when the sperm binds to the egg, before their membranes fuse (*3*). The Na^+ influx produces a fast block of multiple sperm entries (polyspermy), which is lethal to the embryos of many plants and animals (*3*). The shift in the potential of the egg membrane to a positive level during fertilization and the high concentration of ATP in sperm cells initiated our study of the ionic events induced by ATP in *Xenopus laevis* oocytes.

Burnstock (*4*) defined ATP receptors as distinct from adenosine receptors on the basis of their selectivity for ATP. The ATP receptor is a ligand-gated calcium channel in smooth muscle cells (*5*) and in PC 12 cells (*6–8*). When the channel is activated, the inward Ca^{2+} current depolarizes the cell. In neuronal cell bodies purinoceptors of the P_2 type are coupled to nonselective cationic channels (*9*). Studies have demonstrated that the application of ATP to intact *Xenopus* oocytes evokes a depolarizing current response (*10*).

Defolliculated oocytes (*11*) responded to ATP application with a large inward current from 0.1 to 2.5 μA (Fig. 1, inset), consistent with what occurs when cation-conducting channels are opened. The response occurred rapidly (~1 s), reached a peak in 10 to 30 s, and then decayed slowly (2 to 3 min) to the basal level. After the ATP was removed, the current decayed rapidly (1 to 5 s) to the basal level (Fig. 1, inset). The response saturated at an apparent Michaelis constant K_m of 196 ± 74 μM (mean ± SEM, n = 6 normalized determinations) and maximal amplitude of 2.4 ± 0.2 μA (mean ± SEM, Fig. 1). The reversal potential of the ATP response (0.2 mM) in normal ND 96 buffer was −16 ± 3 mV [mean ± SEM, n = 5, Fig. 2A (*12*)]. When we omitted Na^+ from the medium by exchange with *N*-methyl-D-glucamine, the reversal potential shifted to −29 ± 4.2 mV (± SEM, n = 5) and the ATP-activated inward current was reduced throughout the voltage range, indicating that Na^+ was responsible for 80 to 90% of the ATP-induced current (Fig. 2B). Increasing external K^+ to 50 mM shifted the reversal potential to 11 ± 3.3 mV (± SEM, n = 4, Fig. 2C). Omitting Ca^{2+} from the buffer caused no significant change in the reversal potential (−11.2 ± 2.1 mV, ± SEM, n = 4), demonstrating that Ca^{2+} contributed little to the ATP response in the oocyte. In many cells ATP has been shown to activate inositol triphosphate formation (*13*). Therefore, we investigated the possibility that some of the ATP-induced current is mediated by the activation of Cl^- channels which are Ca^{2+}-sensitive. Our results excluded this possibility. The ATP-induced current remained unchanged when methanesulfonic acid was substituted for Cl^- or when oocytes were preinjected with EGTA (*14*).

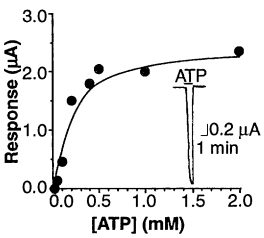

Fig. 1. Response induced by ATP in defolliculated oocytes. The inward current was recorded on bath application of 0.5 mM ATP at −60 mV. The horizontal bar indicates the duration of ATP application (inset). The graph is a dose-response curve of ATP-induced current. We recorded inward currents at a holding potential of −60 mV with increasing ATP concentrations. The curve was fitted by the Easy Fitter program.

The hydrolytic products of ATP (adenosine diphosphate, adenosine monophosphate, and adenosine) were ineffective at inducing a conductance change in *Xenopus* oocytes, indicating that the oocytes had receptors selective for ATP. The absence of any effect of Mg^{2+} on the ATP response suggests that ATP^{4-} is not the active species, as reported for mast cells (*15*). However, externally applied guanosine triphosphate (GTP) was effective at antagonizing the ATP-induced current (dissociation constant of enzyme-inhibitor complex (K_i) of 42 μM, Fig. 3), while GTP alone evoked an inward current only at concentrations >1 mM. The most effective inhibitors of the ATP-mediated conductance change in *Xenopus* oocytes were the nonhydrolyzable GTP analogs guanosine 5′-*O*-(3-thiotriphosphate) (GTP-γ-S) and guanosine 5′-[β,γ-imido]triphosphate (GppNHp). Both were about 10-fold more potent than GTP with an apparent K_i of 3.5 μM and 3.88 μM, respectively (Fig. 3). A pyrimidine nucleotide, uridine triphosphate (UTP), was also effective at antagonizing the ATP-induced response (K_i = 57.6 μM, Fig. 4A), indicating the importance of the hydroxyl group at the 2′-position of the aromatic ring for recognition at the ATP binding site. Another pyrimidine nucleotide with an amino group at the 2′-position, cytidine triphosphate (CTP), did not inhibit the ATP-mediated response (Fig. 4A).

The ATP analog α,β-methylene-ATP, which inhibits the effect of ATP in cardiac myocytes (*16*) and parasympathetic neurons (*17*) but not in skeletal muscle (*18*), did not inhibit the ATP response in *Xenopus*

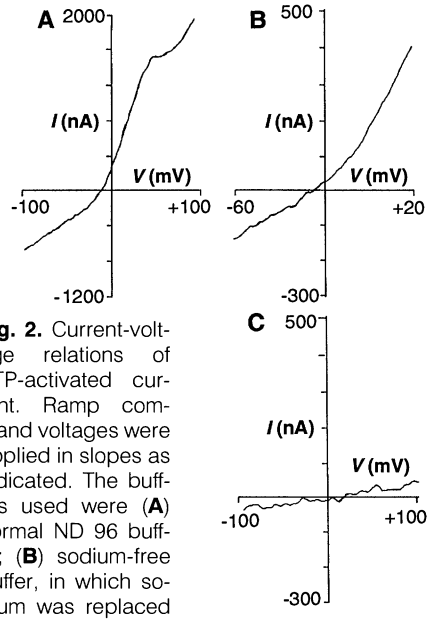

Fig. 2. Current-voltage relations of ATP-activated current. Ramp command voltages were applied in slopes as indicated. The buffers used were (**A**) normal ND 96 buffer; (**B**) sodium-free buffer, in which sodium was replaced by *N*-methyl-D-glucamine (ATP application elevated Na^+ concentration to 0.8 mM because of the Na^+ present for each ATP molecule); and (**C**) ND 96 supplemented with 50 mM KCl.

Department of Biological Chemistry, Hebrew University of Jerusalem, Jerusalem, 91904 Israel.

*To whom correspondence should be addressed.

Fig. 3. Inhibition of the ATP-induced response by GTP and its analogs. We measured ATP-mediated currents in ND 96 buffer. The trisphosphate nucleotides were added to the oocytes in increasing concentrations, as indicated, 1 to 2 min before ATP application. GTP (○), GppNHp (□), GTP-γ-S (●). Current recordings were made at a holding potential of −60 mV. Values are the average ± SEM (n = 3) and are presented as percent of control. The dissociation constants (K_i) were calculated using the Cheng and Prussoff equation (*24*) $K_i = EC_{50}/(1 + [I]/K_m)$, where K_m represents the apparent K_m value for ATP-induced response (Fig. 1), EC_{50} is the concentration needed to inhibit 50% of the response, and [I] is the applied ATP concentration (1 mM for GTP and 0.5 mM for the other two ligands).

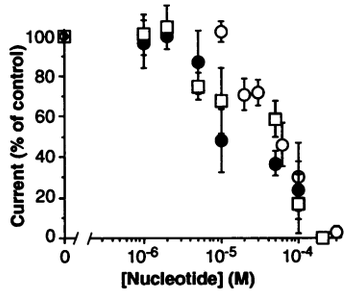

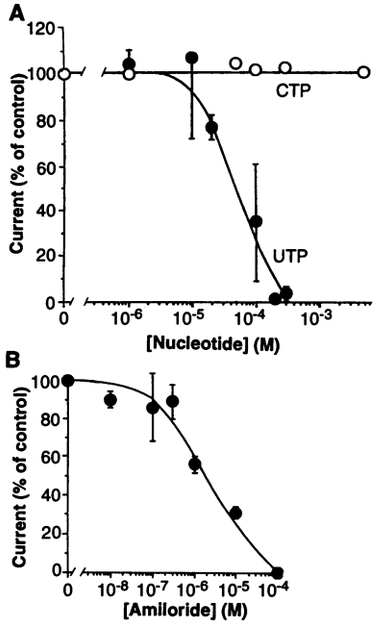

Fig. 4. Inhibition of ATP-induced current by UTP, CTP, and amiloride. We added increasing concentrations of (**A**) UTP (●), CTP (○), or (**B**) amiloride to oocytes at the indicated concentrations 1 to 2 min before applying 0.5 mM ATP. Inward currents were elicited at a holding potential of −60 mV. Values are the average ± SEM (n = 3) presented as percent of control, and the dissociation constants were calculated as described for Fig. 3.

oocytes. Likewise, the nonhydrolyzable ATP analogs adenosine 5′-[β,γ-imido]triphosphate and α,β-methylene-ATP had no depolarizing effect on the oocytes, again showing the high selectivity of the ATP receptor. Reactive blue, Coomassie blue, and suramin did not antagonize the ATP response (*19*), confirming that the ATP receptor of the *Xenopus* oocytes has little structural resemblance to other ATP receptors. Most notable is its high sensitivity to GTP and GTP analogs. Amiloride is a potent inhibitor of the renal Na^+ channels and the Na^+-H^+ antiporter (*20, 21*), and amiloride potently inhibited the ATP-induced current [inhibition concentration (IC_{50}) of 2.12 ± 0.96 μM (mean ± SEM)] (Fig. 4B). Hexamethylene amiloride, an analog of amiloride, also inhibited the ATP response (IC_{50} = 8.7 ± 1.4 μM), supporting the idea that the ATP receptor is a Na^+ current mediator.

The high concentration of ATP in sperm prompted us to explore the possible role of this ATP receptor in fertilization. Mature eggs were squeezed out of *Xenopus* females that had been treated with human chorionic gonadotropin hormone (*22*). The eggs were divided into groups of 15 to 25 and fertilized in the absence or in the presence of either GTP, GppNHp, or amiloride (*22*). Until the beginning of gastrulation, the most visible sign of fertilization is furrow cleavage. This is characterized by a penetration of subcortical plasm into the interior of the egg, particularly at the animal half of the egg (Fig. 5A). Therefore, fertilization was determined by visualizing cleavages (stage 3) in each of the egg groups. Fertilization was strongly inhibited in the presence of GTP, GppNHp, and amiloride (Fig. 5B). Other studies have shown that insemination of sea urchin eggs in the presence of a high amiloride concentration interfered with fertilization (*23*).

The correlation between inhibition of sperm-induced fertilization and inhibition of the ATP-mediated opening of Na^+ channels suggests that ATP receptors on mature eggs bind ATP from sperm and transmit a signal for egg activation. In many species, including the marine worm *Urechis*, sperm initiates a change in potential in the egg membrane, which has been attributed to an increase in Na^+ permeability (*2*). It is possible that in other species activation of the ATP receptor might be an early and essential step in the sequence leading to fertilization.

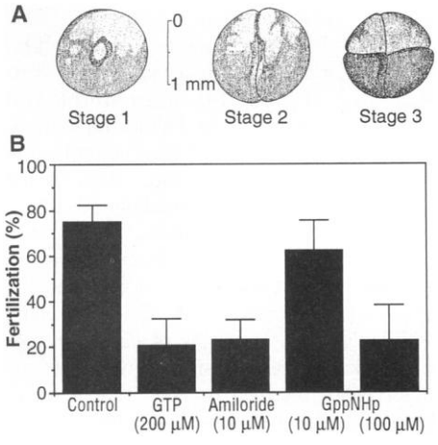

Fig. 5. (**A**) Animal view of the first stages of development after fertilization in *Xenopus* eggs. The cleavages in a fertilized egg at the first, second, and third stages of fertilization are the most visible sign of the developmental process. The furrows are easily seen, especially at the third stage representing a four-cell stage. Magnification, ×10 [adapted from (*25*)]. (**B**) Inhibition of fertilization in *Xenopus* eggs. Primed eggs were fertilized in the absence and in the presence of GTP (200 μM), amiloride (10 μM), or GppNHp (10 and 100 μM) according to the procedure described (*22*). Fertilization was determined by visualizing the cleavage furrows (indentation of the subcortical plasm into the interior of the egg) at the four-cell stage (stage 3, see Fig. 5A). The results represent the average of three independent experiments carried out in duplicates in which each sample contained 15 to 25 eggs. Bars represent standard errors.

REFERENCES AND NOTES

1. S. Hagiwara and L. A. Jaffe, *Annu. Rev. Biophys. Bioeng.* **8**, 385 (1979); L. A. Jaffe, M. Gould-Somero, L. Z. Holland, *J. Gen. Physiol.* **73**, 469 (1979).
2. M. Gould and J. L. Stephano, *Science* **235**, 1654 (1987).
3. M. Gould-Somero, L. A. Jaffe, L. Z. Holland, *J. Cell Biol.* **82**, 426 (1979); H. Schuel and R. Schuel, *Dev. Biol.* **87**, 249 (1981); F. J. Longo, J. W. Lynn, D. H. McCulloh, E. L. Chambers, *ibid.* **118**, 155 (1986).
4. G. Burnstock, in *Cell Membrane Receptors for Drugs and Hormones: A Multidisciplinary Approach*, L. Bollis and R. W. Straub, Eds. (Raven, New York, 1978), pp. 107–118.
5. C. D. Benham, T. B. Bolton, N. G. Byren, W. A. Large, *J. Physiol. (London)* **387**, 473 (1987); C. D. Benham and R. W. Tsien, *Nature* **328**, 275 (1987); P. Sneddon, D. P. Westfall, J. S. Fedan, *Science* **218**, 693 (1982).
6. K. Nakazawa, K. Fujimori, A. Takanaka, K. Inoue, *J. Physiol. (London)* **428**, 257 (1990).
7. D. Sela, E. Ram, D. Atlas, *J. Biol. Chem.* **266**, 17990 (1990).
8. R. Neuhaus, B. F. X. Reber, H. Reuter, *J. Neurosci.* **11**, 3984 (1991).
9. B. P. Bean and D. D. Friel, in *Ion Channels*, T. Naharashi, Ed. (Plenum, New York, 1990), vol. 2, pp. 169–203; B. P. Bean, *Trends Pharmacol. Sci.* **13**, 87 (1992).
10. I. Lotan, N. Dascal, S. Cohen, Y. Lass, *Pfluegers Arch.* **406**, 158 (1986).
11. The largest oocytes (stages 5 and 6) were defolliculated by treatment with collagenase (2 mg/ml) and maintained in ND 96, sterile buffer: 96 mM NaCl, 2 mM KCl, 1 mM $MgCl_2$, 1.8 mM $CaCl_2$, and 5 mM Hepes (pH 7.5). The sterile buffer was supplemented with sodium pyruvate (2.5 mM), penicillin (100 U/ml), and streptomycin (100 μg/ml) at 18°C. The disodium salt of ATP was titrated to pH 7.4 with tris. We recorded whole-cell currents at 20°C with a DAGAN 8500 amplifier. The voltage clamp was maintained with dual (3 M KCl) microelectrodes having an electrode resistance of 1 to 5 megohms. All drugs, agonists, and antagonists were added for 1 to 2 min before stimulation and were prepared in ND 96 buffer immediately before use.
12. Current-voltage (*I-V*) relations for the ATP responses were obtained by the ramp method. A voltage ramp command with slopes of 80 or 200 mV/s were applied to the oocytes. The current

traces, with and without ATP, in response to the voltage ramp were recorded and digitized. Digitized current traces were averaged and subtracted from current traces with ATP opened channels, and the difference was plotted as a function of voltage to yield smooth *I-V* relations. Only oocytes with a resting potential below −30 mV were used.

13. G. Burnstock, *Ann. N.Y. Acad. Sci.* **603**, 1 (1990).
14. The oocytes were injected with 50 nl of 0.4 M EGTA (K^+ salt, pH 7.0) 1 day before testing the ATP response [D. Singer *et al.*, *Science* **253**, 1553 (1991)].
15. B. D. Gomperts and J. M. Fernandez, *Trends Biochem. Sci.* **10**, 414 (1985).
16. D. D. Friel and B. P. Bean, *J. Gen. Physiol.* **91**, 1 (1988).
17. L. A. Fieber and D. J. Adams, *J. Physiol. (London)* **434**, 239 (1991).
18. R. I. Hume and M. J. Honig, *J. Neurosci.* **6**, 681 (1986).
19. So far the most potent antagonist found of the ATP receptor reported here is reactive blue 2 (cibacron blue F3GA), proposed to be a P_{2y}-type ATP receptor antagonist in several systems (*6, 8*). Recently, Coomassie blue, another dye with a planar ring structure, was shown to inhibit the P_{2y}-type ATP receptor in PC 12 cells (K_i = 5 μM) (*7*). Both dyes were ineffective at antagonizing ATP-induced depolarization in oocytes at concentrations of up to 100 μM. Suramin, which inhibits ATP-stimulated catecholamine secretion from PC 12 cells [(*8*); K. Nakazawa, K. Fujimori, A. Takanaka, K. Inoue, *Br. J. Pharmacol.* **101**, 224 (1990)], did not antagonize the ATP-mediated depolarization in oocytes (>10 μM).
20. H. Garty and D. Benos, *Physiol. Rev.* **68**, 309 (1988).
21. T. R. Kleyman and E. J. Crago, *J. Membr. Biol.* **105**, 1 (1988).
22. In vitro fertilization (IVF) of *X. laevis*. One day before IVF, male and female frogs were primed with human chorionic gonadotropin. The eggs were squeezed out directly into buffer A (110 mM NaCl, 2 mM KCl, 1 mM $MgSO_4$, 2 mM $NaHCO_3$, 0.5 mM Na_2HPO_4, and 15 mM tris–acetic acid, pH 7.6). Testes were removed and placed in buffer B (100 mM NaCl, 2 mM KCl, 1 mM $MgSO_4$, 2 mM $CaCl_2$, 1 mM EDTA, and 5 mM Hepes, pH 7.4). The eggs (in groups of 15 to 25) and testes (cut into small pieces) were incubated with GTP (200 μM), GppNHp (10 and 100 μM), and amiloride (10 μM) in buffer A and B, respectively, for 5 min at 23°C. (Testes that were not preincubated with the different antagonists gave the same results.) The buffer was then removed, and the pieces of testes, minced slightly with forceps, were brought into contact with the eggs. After 1.5 min, we added 2 ml of buffer B (diluted 10-fold) to dilute sperm in the fertilization assay and to prevent polyspermy. The jelly coat was removed after 20 min by incubating with 2% cysteine (two incubations of 3 min each, with swirling) followed by immediate washes (five to six) with 10-fold diluted buffer B. Fertilization was visualized under the microscope 120 to 150 min after sperm and egg contact. The first cleavage began 90 to 100 min after fertilization depending on the ambient temperature. The cleavage furrow was clearly visible at the center of the animal half even without removal of the jelly coat. The second cleavage furrow was observed approximately 30 min later, and at the four-cell stage (stage 3), the percent of eggs fertilized was determined in the different egg groups.
23. D. Epel, *Cell Differ. Dev.* **29**, 1 (1990).
24. Y. C. Cheng and W. H. Prusoff, *Biochem. Pharmacol.* **22**, 3099 (1973).
25. P. D. Niewkoop and J. Faber, Eds., *Normal Table of* Xenopus laevis (*Daudin*): *A Systematic and Chronological Survey of the Development From the Fertilized Egg Till the End of Metamorphosis*, (North-Holland, Amsterdam, 1956), p. 244].

26. We thank N. Dascal and O. Wiser for helpful suggestions and the Hebrew University Center for Research on Pain for help in the purchase of instruments.

31 March 1993; accepted 11 May 1993

Subunit Identification and Reconstitution of the N-Type Ca^{2+} Channel Complex Purified from Brain

Derrick R. Witcher, Michel De Waard, Junshi Sakamoto, Clara Franzini-Armstrong, Marlon Pragnell, Steven D. Kahl, Kevin P. Campbell*

Calcium channels play an important role in regulating various neuronal processes, including synaptic transmission and cellular plasticity. The N-type calcium channels, which are sensitive to ω-conotoxin, are involved in the control of transmitter release from neurons. A functional N-type calcium channel complex was purified from rabbit brain. The channel consists of a 230-kilodalton subunit (α_{1B}) that is tightly associated with a 160-kilodalton subunit ($\alpha_2\delta$), a 57-kilodalton subunit (β_3), and a 95-kilodalton glycoprotein subunit. The complex formed a functional calcium channel with the same pharmacological properties and conductance as those of the native ω-conotoxin–sensitive calcium channel in neurons.

In neurons, the calcium influx that triggers vesicle fusion to the presynaptic membrane and subsequent neurotransmitter release is the result of the activation of voltage-sensitive Ca^{2+} channels in the plasma membrane (*1*). Using freeze-fracture electron microscopy, investigators have identified active zone particles in the presynaptic membrane that have been proposed to be voltage-sensitive Ca^{2+} channels (*2*). These Ca^{2+} channels may be the antigen or may be associated with the antigen recognized by pathogenic autoantibodies in small cell lung carcinoma involved in Lambert-Eaton myasthenic syndrome (*3*). The N-type Ca^{2+} channels are distinguished from L-, T-, and P-type voltage-dependent Ca^{2+} channels by electrophysiological and pharmacological properties (*4*). The peptide ω-conotoxin GVIA, isolated from the snail *Conus geographus*, selectively blocks N-type Ca^{2+} channels, whereas the L-type Ca^{2+} channels are inhibited by dihydropyridines (DHPs) (*5*). The DHP-sensitive Ca^{2+} channel from skeletal muscle has been purified and is composed of four subunits: α_1 (molecular weight 175 kD), $\alpha_2\delta$ (160 kD), β (52 kD), and γ (32 kD) (*6*). At least four genes encoding Ca^{2+} channel α_1 subunits from the brain share homology with the α_1 subunit of the skeletal muscle DHP receptor (*7, 8*). Recently, the complementary DNA (cDNA) encoding the human neuronal class B α_1 subunit (*7*) has been transiently expressed to produce ω-conotoxin–sensitive currents (*9*). Although there has been recent progress in molecular biological studies of brain Ca^{2+} channel subunits (*7, 8*), little is known about the native structure and function of neuronal Ca^{2+} channels.

We have purified the ω-conotoxin receptor (N-type Ca^{2+} channel) from digitonin-solubilized rabbit brain membranes by heparin chromatography, immunoaffinity chromatography, and sucrose density gradient centrifugation (*10*). The receptor complex migrated as a single peak on the sucrose density gradient (Fig. 1A) and contained four subunits of molecular weight 230 kD, 140 kD (reduced), 95 kD, and 57 kD, all of which comigrated with the peak of binding to ^{125}I-labeled ω-conotoxin (Fig. 1B) and were in a stoichiometric ratio of 1:1.0:0.9:1.3. In more than 70 purifications, these four subunits were consistently observed.

The isolated ω-conotoxin receptors appeared as globular complexes (Fig. 1C). Most of the complexes were within a narrow size range, indicating the purity of the preparation. The approximate diameter was 16 nm, which is similar to the size of active zone particles in the presynaptic membranes, as visualized by freeze-fracture electron microscopy (*2*). The few larger complexes in each image were possibly aggregates of receptors.

Rabbit brain membranes bound ^{125}I-labeled ω-conotoxin with a dissociation constant (K_d) of 0.08 nM, in agreement with other reports (*11, 12*), and a maximum binding capacity (B_{max}) of 305 fmol per milligram of protein. A 2400-fold purification of the receptor was achieved, yielding 60 μg of purified N-type Ca^{2+} channel. The purified receptor bound ^{125}I-labeled ω-conotoxin with a K_d of 0.06 nM and a B_{max} of 423 pmol/mg (Fig. 1D); however, it did not bind [^{3}H]PN200-110, a specific blocker of L-type Ca^{2+} channels. Only a single binding site was observed for ω-conotoxin both in brain membranes and for the purified receptor.

To confirm the subunit composition of the receptor, we generated sheep antibodies

D. R. Witcher, M. De Waard, J. Sakamoto, S. D. Kahl, K. P. Campbell, Howard Hughes Medical Institute, Department of Physiology and Biophysics, University of Iowa College of Medicine, Iowa City, IA 52242.
C. Franzini-Armstrong, Department of Anatomy, University of Pennsylvania, Philadelphia, PA 19104.
M. Pragnell, Program in Neuroscience, University of Iowa College of Medicine, Iowa City, IA 52242.

*To whom correspondence should be addressed.